

Trinuclear Lanthanoid Complexes of 1,3,5-Triamino-1,3,5-trideoxy-*cis*-inositol with a Unique, Sandwich-Type Cage Structure¹

Roman Hedinger,^{2a} Michele Ghisletta,^{2a} Kaspar Hegetschweiler,^{*,2b} Eva Tóth,^{2c}
 André E. Merbach,^{2c} Roberta Sessoli,^{2d} Dante Gatteschi,^{2d} and Volker Gramlich^{2e}

Laboratorium für Anorganische Chemie, ETH Zentrum, CH-8092 Zürich, Switzerland,
 Universität des Saarlandes, Fachrichtung Anorganische Chemie, Postfach 15 11 50,
 D-66041 Saarbrücken, Germany, Institut de Chimie Minérale et Analytique, Université de Lausanne—
 BCH, CH-1015 Lausanne, Switzerland, Dipartimento di Chimica, Università di Firenze,
 50144 Florence, Italy, and Institut für Kristallographie, ETH Zentrum, CH-8092 Zürich, Switzerland

Received June 18, 1998

A variety of trinuclear complexes $[M_3(H\text{-}_3L)_2]^{3+}$ [$M = Y, La, Eu, Gd, Dy$; $L = 1,3,5\text{-triamino-1,3,5-trideoxy-}cis\text{-inositol (taci)}$ and $1,3,5\text{-trideoxy-1,3,5-tris(dimethylamino)-}cis\text{-inositol (tdci)}$] was prepared as solid materials of the composition $M_3(H\text{-}_3L)_2X_3 \cdot pH_2O \cdot qEtOH$ ($X = Cl, NO_3$; $2.5 \leq p \leq 9$; $q = 0, 0.33$) and characterized by elemental analyses, NMR spectroscopy, and FAB⁺ mass spectrometry. The crystal structures of $[La_3(H\text{-}_3taci)_2(H_2O)_4Cl]Cl_2 \cdot 3H_2O$ and $[Gd_3(H\text{-}_3taci)_2(H_2O)_6]Cl_3 \cdot 3H_2O$ were elucidated by single-crystal X-ray diffraction studies. The La complex crystallizes in the orthorhombic space group *Pbca*, $a = 17.10(2)$ Å, $b = 16.20(4)$ Å, $c = 20.25(4)$ Å, $Z = 8$ for $C_{12}Cl_3H_{38}La_3N_6O_{13}$. The Gd complex crystallizes in the monoclinic space group *P2₁/n*, $a = 10.294(3)$ Å, $b = 15.494(5)$ Å, $c = 19.994(6)$ Å, $\beta = 95.36(2)^\circ$, $Z = 4$ for $C_{12}Cl_3Gd_3H_{42}N_6O_{15}$. The two complexes exhibited a unique, sandwich-type cage structure, where the two triply deprotonated taci ligands encapsulate an equilateral triangle of the three metal centers. The metal cations are coordinated to the equatorial, terminal amino groups and are bridged by the axial μ_2 -alkoxo groups. The coordination spheres are completed by additional peripheral ligands such as H₂O or Cl[−] counterions. The coordination number of the metal cations is 8. Magnetic susceptibility measurements of the Gd complex revealed very weak antiferromagnetic coupling interactions between the three Gd centers. Complex formation and species distribution in aqueous solution was investigated by potentiometry and pD-dependent NMR spectroscopy. An exclusive formation of the $[Eu_3(H\text{-}_3taci)_2]^{3+}$ unit in solution was found in the range $7 \leq pH \leq 10$. The formation constants were determined for the Y, Eu, Gd, Dy, and Lu complexes with taci. The stability of the lanthanoid complexes increased monotonically with decreasing ionic radius of the metal center.

Introduction

The coordination chemistry of trivalent lanthanoid cations has been thoroughly investigated over the last twenty years due to their potential applications in a variety of important areas. Lanthanoid complexes have interesting luminescence properties,³ and they have been studied as efficient catalysts for the hydrolysis of DNA.⁴ Dy³⁺ and Tm³⁺ complexes are used as shift reagents in NMR spectroscopy.⁵ The solution properties of Gd^{III} complexes are of interest with regard to their application as paramagnetic contrast agents for magnetic resonance imaging (MRI).⁶ A variety of prerequisites must be fulfilled for their

successful use as contrast agents, such as sufficient selectivity of the ligand for Gd^{III}, and high stability of the complex in physiological media. Moreover, suitable biodistribution properties and low toxicity are essential. For an efficient contrast agent, the ability to decrease the relaxation time of the surrounding water protons is the key property. This ability is governed by several parameters, involving the number of inner sphere water molecules, the rate of water exchange, rotation, and electronic relaxation. Currently, Gd^{III} complexes with polyamino polycarboxylates such as 1,4,7,10-tetraazacyclododecane-*N,N',N'',N'''*-tetraacetate (dota), diethylenetrinitriolpentaacetate (dtpa), and diethylenetrinitriolpentaacetate-bis(methyl)amide (dtpa-bma) are used as contrast agents for MRI.

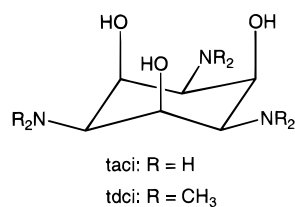
In an extended investigation, it has been shown that 1,3,5-triamino-1,3,5-trideoxy-*cis*-inositol (taci, Chart 1), a cyclohex-

* To whom correspondence should be addressed.

- (1) 1,3,5-Triamino-1,3,5-trideoxy-*cis*-inositol, a Ligand with a Remarkable Versatility for Metal Ions. 9. Part 8: see ref 7.
- (2) (a) Laboratorium für Anorganische Chemie, ETH Zürich. (b) Universität des Saarlandes. (c) Université de Lausanne. (d) Università di Firenze. (e) Institut für Kristallographie, ETH Zürich.
- (3) (a) Richardson, F. S. *Chem. Rev.* **1982**, 82, 541. (b) Frey, S. T.; Chang, C. A.; Carvalho, J. F.; Varadarajan, A.; Schultze, L. M.; Pounds, K. L.; Horrocks, W. D., Jr. *Inorg. Chem.* **1994**, 33, 2882.
- (4) Rammo, J.; Schneider, H.-J. *Liebigs Ann.* **1996**, 1757 and references therein.
- (5) (a) Sink, R. M.; Buster, D. C.; Sherry, A. D. *Inorg. Chem.* **1990**, 29, 3645. (b) Buster, D. C.; Castro, M. M. C. A.; Gerald, C. F. G. C.; Malloy, C. R.; Sherry, A. D.; Siemers, T. C. *Magn. Reson. Med.* **1990**, 15, 25. (c) Bansal, N.; Germann, M. J.; Lazar, I.; Malloy, C. R.; Sherry, A. D. *J. Magn. Reson. Imaging* **1992**, 2, 385.

- (6) (a) Lauffer, R. B. *Chem. Rev.* **1987**, 87, 901. (b) Moonen, C. T. W.; van Zijl, P. C. M.; Frank, J. A.; Le Bihan, D.; Becker, E. D. *Science* **1990**, 250, 53. (c) Kumar, K.; Chang, C. A.; Tweedle, M. F. *Inorg. Chem.* **1993**, 32, 587. (d) Peters, J. A.; Huskens, J.; Raber, D. J. *Prog. Nucl. Magn. Reson. Spectrosc.* **1996**, 28, 283. (e) Micskei, K.; Powell, D. H.; Helm, L.; Brücher, E.; Merbach, A. E. *Magn. Reson. Chem.* **1993**, 31, 1011. (f) González, G.; Powell, D. H.; Tissières, V.; Merbach, A. E. *J. Phys. Chem.* **1994**, 98, 53. (g) Powell, D. H.; Ni Dhubghaill, O. M.; Pubanz, D.; Helm, L.; Lebedev, Y. S.; Schlaepfer, W.; Merbach, A. E. *J. Am. Chem. Soc.* **1996**, 118, 9333. (h) Aime, S.; Botta, M.; Crich, S. G.; Giovenzana, G. B.; Jommi, G.; Pagliarini, R.; Sisti, M. *Inorg. Chem.* **1997**, 36, 2992.

Chart 1



ane-based polyamino polyalcohol, has some rather remarkable metal binding properties.⁷ During the course of this study, we found that the trivalent lanthanoid cations form trinuclear complexes of the composition $[M_3(H-3taci)_2(H_2O)_6]^{3+}$ in aqueous solution.⁸ The Gd^{III} complex could be of particular interest in the context of MRI, due to its compact structure, the high amount of paramagnetism induced by the three Gd^{III} centers, and the six water ligands which are attached to the three Gd^{III} centers. We report here the preparation and characterization of the trinuclear Y^{III}, La^{III}, Eu^{III}, Gd^{III}, and Dy^{III} complexes. Spectroscopic techniques and magnetic susceptibility measurements were used to characterize these complexes. Single-crystal X-ray diffraction studies of the La^{III} and Gd^{III} complexes are presented, and the stability and species distribution in aqueous solution are discussed in detail. For comparison, additional experiments with the methylated derivative 1,3,5-tris(dimethylamino)-*cis*-inositol (tdci, Chart 1) are also reported. The elucidation of the number of inner sphere water molecules in solution, the kinetics of water exchange, and the rotational and EPR properties of these complexes are the subject of an independent paper.⁸

Experimental Section

Materials and Analyses. YCl₃·6H₂O, LaCl₃·7H₂O, EuCl₃·6H₂O, GdCl₃·6H₂O, DyCl₃·6H₂O, LuCl₃·6H₂O were commercially available materials of highest possible quality. NEt₃ and the organic solvents were of reagent grade and were used without further purification. The ligands taci and tdc were prepared according to published procedures.^{9,10} C, H, N, Cl analyses were performed by D. Manser and M. Schneider (Laboratorium für Organische Chemie, ETH-Zürich). Metal analyses (Y, La, Eu, Gd, Dy) were performed by K. Hametner (ETH Zürich) using ICP-OES.

Potentiometry. Potentiometric titrations were performed under an atmosphere of N₂ at 25.0 ± 0.1 °C in 0.1 M aqueous KCl as described previously.¹¹ An Orion 720 A pH meter and a Philips CA 14/02 glass electrode with a built-in Ag/AgCl reference electrode was used for the measurements. The system was calibrated by acid-base titrations¹¹ prior to and after each experiment. Data were only considered when the shift in E^0 was less than 1 mV and when the value of pK_w fell in the range 13.78–13.80. Standardized 0.1 M KOH was dispensed from a Metrohm 665 Dosimat piston buret. The continuous titrations were performed using a sample volume of 50.00 mL and a computer controlled device for data collection and for addition of titrant.¹² A back-titration with 0.1 M HCl was performed after each experiment to check whether complete equilibration had been achieved, and the data were rejected, if a hysteresis in pH could be observed. In this case, a batch method

was applied,^{11,13} using individually sealed sample solutions. The solutions were measured in intervals of 48 h until the pH was found to be constant.

Data were evaluated using the computer program SUPERQUAD,¹⁴ and double checked by the computer program BEST.¹⁵ All equilibrium constants are expressed on the basis of molar concentrations rather than activities. Fixed values were used for pK_w (13.79),¹⁶ the acidity constants of taci ($pK_1 = 5.95$, $pK_2 = 7.40$, $pK_3 = 8.90$)¹⁷ and tdc ($pK_1 = 5.89$, $pK_2 = 7.62$, $pK_3 = 9.68$),¹³ and the total concentrations of metal, ligand, and acid. The listed uncertainties correspond to the standard deviations estimated by SUPERQUAD, multiplied with a factor of 3.

Magnetic Measurements. The magnetization of the Gd complex was measured using a Metronique Ing. MS02 SQUID magnetometer in the temperature range of 2.3–60 K with a static magnetic field H of 10 kOe above 20 K and of 1 kOe below 20 K to avoid saturation effects. The data were corrected for the contribution of the sample holder and for the diamagnetism of the sample using Pascal's constants.

Spectroscopy and Mass Spectrometry. ¹H and ¹³C NMR spectra were measured on a Bruker AMX 500 spectrometer (500.13 and 125.9 MHz for ¹H and ¹³C, respectively). Two-dimensional NMR experiments were performed according to the literature.¹⁸ Chemical shifts (δ , in ppm) are given relative to 3-(trimethylsilyl)propionate-*d*₄ (= 0 ppm) or *t*-butanol (Eu complexes: ¹H, 1.25 ppm; ¹³C, 31.2 ppm). pD (= pH + 0.42)¹⁹ was measured with a glass electrode (Philips).

The FAB⁺ mass spectrometry was performed on a VG ZAB-VSEQ spectrometer, equipped with a VG-Cs⁺ FAB gun (35 keV, 2 μ A beam current). The samples were dissolved in MeOH, and the measurements were made in a 3-nitrobenzyl alcohol (NBA) matrix. Only the most intense metal-containing ions are listed in the Experimental Section. A more comprehensive compilation of mass spectrometric data is presented in Table S13 (Supporting Information).

Preparation of Metal Complexes. Solid trichloride salts of the taci complexes were prepared by the following standard procedure: 177 mg (1.0 mmol) of taci was suspended in about 10 mL of MeOH. NEt₃ (420 μ L, 3.0 mmol) and the hydrated trichloride salt of the metal (1.5 mmol) were added, and the mixture was refluxed. A white solid formed. The suspension was allowed to cool and was then kept at 4 °C. The solid was separated by filtration, washed with cold MeOH, and recrystallized from H₂O/EtOH.

[Y₃(H-3taci)₂]Cl₃·7.5H₂O·0.33EtOH. Yield: 44%. Anal. Calcd for C_{12.666}Cl₃H₄₁N₆O_{13.833}Y₃: C, 17.45; H, 4.74; N, 9.64; Y, 30.59. Found: C, 17.52; H, 4.83; N, 9.70; Y, 30.48. FAB⁺ MS: m/z 684.8 ([Y₃(H-3taci)₂Cl₂]⁺). ¹H NMR (D₂O, pD 7.4): 1.18 (t, EtOH), 3.06 (t, 3 H-C_N), 3.65 (q, EtOH), 4.06 (t, 3 H-C_O). ¹³C NMR (D₂O, pD 7.4): 54.6 (C_N), 73.2 (C_O).

[La₃(H-3taci)₂]Cl₃·9H₂O·0.33EtOH. Yield: 51%. Anal. Calcd for C_{12.666}Cl₃H₄₄La₃N₆O_{15.333}: C, 14.50; H, 4.23; N, 8.01; Cl, 10.14; La, 39.73. Found: C, 14.66; H, 4.08; N, 8.07; Cl, 10.10; La, 39.70. FAB⁺ MS: m/z 834.7 ([La₃(H-3taci)₂Cl₂]⁺). ¹H NMR (D₂O, pD 7.6): 1.18 (t, EtOH), 3.08 (t, 3 H-C_N of complex), 3.19 (m, 3 H-C_N of free taci) 3.65 (q, EtOH), 4.08 (m, 3 H-C_O of free taci), 4.22 (m, 3 H-C_O of complex). The ratio of free to complexed taci is 1:2.5. ¹³C NMR (D₂O, pD 7.6): 51.0 (C_N of taci), 56.0 (C_N of complex), 70.5 (C_O of taci), 74.6 (C_O of complex). Single crystals of the composition [La₃(H-3taci)₂(H₂O)₄Cl]Cl₂·3H₂O suitable for X-ray diffraction studies were grown by layering an aqueous solution of the complex with EtOH.

- (7) Ghisletta, M.; Hausherr-Primo, L.; Gajda-Schranz, K.; Machula, G.; Nagy, L.; Schmalte, H. W.; Rihs, G.; Endres, F.; Hegetschweiler, K. *Inorg. Chem.* **1998**, *37*, 997 and references therein.
 (8) Tóth, É.; Helm, L.; Merbach, A. E.; Hedinger, R.; Hegetschweiler, K.; Jánosy, A. *Inorg. Chem.* **1998**, *37*, 4104.
 (9) Ghisletta, M.; Jalett, H.-P.; Gerfin, T.; Gramlich, V.; Hegetschweiler, K. *Helv. Chim. Acta* **1992**, *75*, 2233.
 (10) Hegetschweiler, K.; Ermi, I.; Schneider, W.; Schmalte, H. *Helv. Chim. Acta* **1990**, *73*, 97.
 (11) Kradolfer, T.; Hegetschweiler, K. *Helv. Chim. Acta* **1992**, *75*, 2243.
 (12) Kissner, R. *AUTOTIT*, Version 2.3: *Computer Program for Control of pH-metric Titrations*; ETH Zürich: Switzerland, 1995.

- (13) Hegetschweiler, K.; Kradolfer, T.; Gramlich, V.; Hancock, R. D. *Chem. Eur. J.* **1995**, *1*, 74.
 (14) Gans, P.; Sabatini, A.; Vacca, A. *J. Chem. Soc., Dalton Trans.* **1985**, 1195.
 (15) Motekaitis, R. J.; Martell, A. E. *Can. J. Chem.* **1982**, *60*, 2403.
 (16) Martell, A. E.; Smith, R. M.; Motekaitis, R. J. *Critically Selected Stability Constants of Metal Complexes. NIST Standard Reference Database 46*, Version 4.0; NIST Standard Reference Data, NIST: Gaithersburg, MD 20899, 1997.
 (17) Hegetschweiler, K.; Gramlich, V.; Ghisletta, M.; Samaras, H. *Inorg. Chem.* **1992**, *31*, 2341.
 (18) (a) Bax, A.; Subramanian, S. *J. Magn. Reson.* **1986**, *67*, 565. (b) Bax, A.; Summers, M. F.; *J. Am. Chem. Soc.* **1986**, *108*, 2093.
 (19) (a) Glasoe, P. K.; Long, F. A. *J. Phys. Chem.* **1960**, *64*, 188. (b) Delgado, R.; Fraústo Da Silva, J. J. R.; Amorim, M. T. S.; Cabral, M. F.; Chaves, S.; Costa, J. *Anal. Chim. Acta* **1991**, *245*, 271.

Anal. Calcd for $C_{12}Cl_3H_{38}La_3N_6O_{13}$: C, 14.45; H, 3.84; N, 8.42. Found: C, 14.71; H, 3.98; N, 8.30.

[Eu₃(H₋₃taci)₂]Cl₃·9H₂O. Yield: 17%. Anal. Calcd for $C_{12}Cl_3$ - $Eu_3H_{42}N_6O_{15}$: C, 13.44; H, 3.95; N, 7.83; Eu, 42.50. Found: C, 13.39; H, 3.87; N, 7.67; Eu, 42.26. FAB⁺ MS: m/z 874.7 ([Eu₃(H₋₃taci)₂Cl₂]⁺). ¹H NMR (D₂O, pD 7.4): -14.63 (br, 3 H-C_O), -21.69 (br, 3 H-C_N).²⁰ ¹³C NMR (D₂O, pD 7.4): 45.5 (C_N), 167.8 (C_O).²⁰ Drying of this product for 2 days over P₂O₅ at 0.05 mbar resulted in the formation of [Eu₃(H₋₃taci)₂]Cl₃·3H₂O. Anal. Calcd for $C_{12}Cl_3Eu_3H_{30}N_6O_9$: C, 14.94; H, 3.13; N, 8.71; Cl, 11.03; Eu, 47.26. Found: C, 15.02; H, 3.16; N, 8.47; Cl, 10.74; Eu, 46.0.

[Gd₃(H₋₃taci)₂]Cl₃·9H₂O. Yield: 14%. Anal. Calcd for $C_{12}Cl_3$ - $Gd_3H_{42}N_6O_{15}$: C, 13.24; H, 3.89; N, 7.72; Gd, 43.34. Found: C, 13.38; H, 3.82; N, 7.72; Gd, 43.02. FAB⁺ MS: m/z 891.0 ([Gd₃(H₋₃taci)₂Cl₂]⁺). Single crystals of the composition [Gd₃(H₋₃taci)₂(H₂O)₆]Cl₃·3H₂O suitable for X-ray diffraction studies were grown by layering an aqueous solution of the complex with EtOH. Anal. Calcd for $C_{12}Cl_3$ - $Gd_3H_{42}N_6O_{15}$: C, 13.24; H, 3.89; N, 7.72. Found: C, 13.31; H, 3.87; N, 7.68.

[Dy₃(H₋₃taci)₂]Cl₃·6H₂O·0.33EtOH. Yield: 54%. Anal. Calcd for $C_{12.666}Cl_3Dy_3H_{38}N_6O_{12.333}$: C, 14.28; H, 3.59; N, 7.89; Dy, 45.75. Found: C, 14.29; H, 3.48; N, 7.85; Dy, 45.74. FAB⁺ MS: m/z 906.9 ([Dy₃(H₋₃taci)₂Cl₂]⁺).

[Eu₃(H₋₃tdci)₂](NO₃)₃·7H₂O. Eu₂O₃ (0.50 g, 1.42 mmol) was suspended in 20 mL of H₂O. Aqueous 1 M HNO₃ (8.62 mL, 8.62 mmol) was added, and the suspension was refluxed for 30 min. The clear solution was evaporated to a total volume of about 2 mL, transferred quantitatively to a volumetric flask, and diluted to a total volume of exactly 10.0 mL. A 0.75 mL amount of this solution (0.21 mmol Eu) was added to a solution of tdc1 (41 mg, 0.16 mmol) in 0.5 mL of H₂O. The solution was refluxed for 1 h. A white solid formed. The suspension was allowed to stand for 2 days at 4 °C. The solid (16.5 mg, 16%) was filtered off, washed with cold water, and dried in air. Anal. Calcd for $C_{24}Eu_3H_{62}N_9O_{22}$: C, 22.44; H, 4.86; N, 9.81. Found: C, 22.42; H, 4.75; N, 9.75. FAB⁺ MS: 1097.3 ([Eu₃(H₋₃tdci)₂(NO₃)₂]⁺). The complex is not sufficiently soluble for NMR measurements. NMR data were sampled from a solution of EuCl₃·6H₂O and tdc1 in a 3:2 molar ratio using NaOD to adjust the pD to 8.5. ¹H NMR (D₂O, pD 8.5): -15.19 (3 H-C_N), -11.70 (3 H-C_O), -4.54 (18 CH₃). ¹³C NMR (D₂O, pD 8.5): 58.3 (C_N), 63.7 (CH₃), 181.1 (C_O). The same method was used for the assignment as described for the corresponding taci complex.²⁰ Single crystals of the composition [Eu₃(H₋₃tdci)₂(H₂O)₂(NO₃)₂]⁺·H₂O were grown from CH₃CN/H₂O.²¹

[Eu₃(H₋₃taci)₂(H₂O)₆](NO₃)₃·3H₂O was prepared by a related procedure, using a 0.2 M Eu(NO₃)₃ solution and solid taci. In addition, the pH was adjusted to 7.6 with KOH. Single crystals were grown from EtOH/H₂O. The compound showed the same NMR characteristics as [Eu₃(H₋₃taci)₂]Cl₃·9H₂O.²²

(20) The assignments for [Eu₃(H₋₃taci)₂]³⁺ were performed by a spin saturation transfer experiment, using an equilibrated D₂O solution, containing comparable amounts of the Eu complex and free ligand. Irradiation at the frequency of the proton resonance H-C_O of the free ligand resulted in the disappearance of the signal at -14.63 ppm. Vice versa, saturation of the H-C_N resonance of the free ligand resulted in the disappearance of the signal at -21.69 ppm. The two ¹³C resonances at 45.5 (C_N) and 167.8 ppm (C_O) were assigned by a ¹H - ¹³C HMQC experiment (ref 18). The assignment for the two protons of the free ligand is from ref 10 and is in agreement with the difference in *T*₁ reported in ref 34.

(21) A low-quality single-crystal X-ray diffraction study of [Eu₃(H₋₃tdci)₂(H₂O)₂(NO₃)₃]⁺·H₂O was performed. Crystal data: space group *P*₂₁/*n* (monoclinic), *a* = 22.963(13) Å, *b* = 17.266(6) Å, *c* = 25.25(2) Å, β = 114.38°, *Z* = 4 (for C₄₈H₁₀₆Eu₆N₁₈O₃₅), *R* = 13.1% for all 6686 unique reflections and 464 refined parameters (on *F*², Syntex P21 four-circle diffractometer, graphite-monochromated Mo Kα radiation). Due to the poor crystal quality, the data set was not of sufficient quality for publication. It allowed, however, an unambiguous elucidation of the connectivity in the trinuclear [Eu₃(H₋₃tdci)₂]³⁺ cage structure. H₂O and NO₃⁻ are coordinated as peripheral ligands to the Eu centers. Two of the six NO₃⁻ ions showed bridging interactions between two adjacent trinuclear complex entities, exhibiting a bidentate and a monodentate coordination mode, respectively. The coordination number of Eu is 9, the mean Eu...Eu distance is 3.745 Å.

Table 1. Crystallographic Data for [La₃(H₋₃taci)₂(H₂O)₄]Cl₂·3H₂O and [Gd₃(H₋₃taci)₂(H₂O)₆]Cl₃·3H₂O

	La complex	Gd complex
empirical formula	C ₁₂ Cl ₃ H ₃₈ La ₃ N ₆ O ₁₃	C ₁₂ Cl ₃ Gd ₃ H ₄₂ N ₆ O ₁₅
fw	997.58	1088.61
space group	<i>Pbca</i> (No. 61)	<i>P</i> ₂ ₁ / <i>n</i> (No. 14)
<i>a</i> , Å	17.10(2)	10.294(3)
<i>b</i> , Å	16.20(4)	15.494(5)
<i>c</i> , Å	20.25(4)	19.994(6)
β, deg	90	95.36(2)
<i>V</i> , Å ³	5610(19)	3175(2)
<i>Z</i>	8	4
<i>T</i> , °C	20(2)	20(2)
λ (Mo Kα), Å	0.710 73	0.710 73
ρ _{calc} , g cm ⁻³	2.36	2.28
μ, cm ⁻¹ (Mo Kα)	48.39	65.16
<i>R</i> [<i>I</i> > 2σ(<i>I</i>)] ^a	0.041	0.028
<i>R</i> _w [<i>I</i> > 2σ(<i>I</i>)] ^b	0.046	0.036

$$^a R = \sum ||F_o| - |F_c|| / \sum |F_o|. \quad ^b R_w = [\sum w(|F_o| - |F_c|)^2 / \sum w F_o^2]^{1/2}.$$

[Y₃(H₋₃tdci)₂(NO₃)₃]⁺·7.5H₂O was prepared analogously from tdc1 (0.19 mmol) and aqueous Y(NO₃)₃ (0.29 mmol). Yield: 19%. Anal. Calcd for $C_{24}H_{63}N_9O_{22.5}Y_3$: C, 26.10; H, 5.75; N, 11.41; Y, 24.15. Found: C, 26.27; H, 5.80; N, 11.45; Y, 23.71. FAB⁺ MS: 907.1 ([Y₃(H₋₃tdci)₂(NO₃)₂]⁺). ¹H NMR (CD₃OD): 1.71 (m, 3 H-C_N), 2.43 (s, 18 H, N-CH₃), 4.64 (m, 3 H-C_O). ¹³C NMR (D₂O, pD 7.4): 43.1 (CH₃), 66.1 (C_O), 71.1 (C_N).

Single-Crystal X-ray Diffraction Studies. Crystallographic data are listed in Table 1. A summary of selected bond lengths and angles is given in Table 2.

Diffraction data of the La complex were sampled on a Picker-Stoe four-circle diffractometer using a colorless crystal having approximate dimensions of 0.3 × 0.4 × 0.6 mm and graphite monochromated Mo Kα radiation. Of 4118 reflections collected, 3674 were unique and 3187 were observed with *I* > 2σ(*I*). Checking of standard reflections during data collection indicated no significant loss of intensity (<5%). The data were corrected for Lorentz and polarization effects and a numerical, face-indexed absorption correction was applied with min and max transmission coefficients of 0.0945 and 0.2758, respectively. The structure was solved by direct methods (SHELXTL PLUS).²³ All hydrogen atoms of the complex molecule could be located in a difference Fourier map. They were included in the refinement at calculated positions (riding model) with fixed isotropic displacement parameters of 0.08 Å². The non-hydrogen atoms were all refined in the anisotropic mode. A total of 334 parameters was varied in the final refinement using full-matrix least-squares calculations (on *F*).²³

Diffraction data of the Gd complex were collected on a Syntex P21 four-circle diffractometer using a colorless crystal having approximate dimensions of 0.30 × 0.15 × 0.10 mm and graphite-monochromated Mo Kα radiation. Checking of standard reflections indicated no significant loss of intensity during the measurement (<2%). Of 4307 intensities measured, 4171 were unique and 3478 were observed with *I* > 2σ(*I*). The data were corrected for Lorentz and polarization effects and a numerical, face-indexed absorption correction was applied with min and max transmission coefficients of 0.4065 and 0.5482, respectively. The structure was solved by direct methods (SHELXTL PLUS).²³ All hydrogen atoms of the complex molecule could be located in a difference Fourier map. They were included in the refinement at calculated positions (riding model) with fixed isotropic displacement parameters of 0.05 Å². The non-hydrogen atoms were all refined in

(22) [Eu₃(H₋₃taci)₂(H₂O)₆](NO₃)₃·3H₂O. Space group *P*₂₁/*2*₁ (orthorhombic), *a* = 10.710(9) Å, *b* = 15.837(12) Å, *c* = 19.23(2) Å, *Z* = 4 (for C₁₂H₄₂Eu₃N₉O₂₄), *R* = 4.49% for 1519 observed reflections with *I* > 2σ(*I*) and 280 refined parameters (on *F*, Syntex P21 four-circle diffractometer, graphite-monochromated Mo Kα radiation). The structure of the discrete [M₃(H₋₃taci)₂(H₂O)₆]³⁺ cations is virtually identical for Eu and Gd. The mean Eu...Eu distance is 3.753 Å; see Hedinger, R. Thesis, Diss. ETH No. 12611, Zürich, Switzerland, 1998.

(23) Sheldrick, G. M. *SHELXTL-PLUS 88. Structure Determination Software Programs*; Nicolet Instrument Corp.: Madison, WI, 1988.

Table 2. Selected Bond Lengths (Å) and Angles^a (deg) of [La₃(H₋₃taci)₂(H₂O)₄Cl]Cl₂·3H₂O and [Gd₃(H₋₃taci)₂(H₂O)₆]Cl₃·3H₂O with ESDs in Parentheses

	La complex		Gd complex	
	range	mean	range	mean
M···M	3.922(1)–3.943(1)	3.931	3.718(1)–3.743(1)	3.734
M–O _{taci}	2.384(8)–2.496(8)	2.443	2.295(6)–2.378(6)	2.343
M–OH ₂	2.533(8)–2.654(8)	2.604	2.422(7)–2.463(7)	2.443
M–N	2.659(10)–2.743(11)	2.697	2.575(8)–2.611(8)	2.592
M–Cl	2.923(4)–2.947(4)	2.935		
M···M···M	59.8(1)–60.3(1)	60.0	59.6(1)–60.2(1)	60.0
N–M–O	64.6(3)–67.9(3)	65.6	65.4(2)–68.7(2)	67.3
N–M–O'	128.7(3)–132.8(3)	130.3	130.0(2)–133.6(2)	131.5
N–M–N'	155.5(3)–157.1(3)	156.4	151.0(3)–151.6(3)	151.3
N–M–OH ₂	76.9(3)–86.5(3)	81.9	75.2(3)–83.1(3)	79.1
O–M–O	73.9(3)–76.2(3)	75.6	77.0(2)–79.9(2)	78.1
O–M–O' (cis)	64.8(3)–66.9(3)	65.7	65.2(2)–65.9(2)	65.6
O–M–O' (trans)	108.3(3)–111.9(3)	109.7	108.0(2)–114.6(2)	112.4
O–M–OH ₂ (cis)	81.0(3)–112.6(3)	92.3	88.4(2)–96.3(2)	91.2
O–M–OH ₂ (trans)	137.4(3)–151.0(3)	144.8	142.4(2)–151.0(2)	146.1
H ₂ O–M–OH ₂		71.6(3)	78.6(3)–82.6(3)	80.1
M–O–M	106.1(3)–109.5(3)	107.1	103.9(2)–108.3(2)	105.7
M–O–C	117.6(7)–121.1(7)	119.3	118.2(5)–121.4(5)	119.4
M–N–C	99.2(7)–101.4(7)	100.1	99.3(5)–101.2(5)	100.0

^a Intraligand angles are indicated as X–M–Y, interligand angles as X–M–Y' (X, Y = N, O).

the anisotropic mode. A total of 370 parameters were varied in the final full-matrix least-squares calculations (on *F*).²³ It appeared, however, that the distance between O(3w) and O(5w) was unusually short (2.06 Å) and that the oxygen positions of O(2w), O(3w), O(4w), and O(5w) had rather large displacement parameters. This result was interpreted in terms of a disorder with a partial occupancy (50%) of these water positions. This interpretation is consistent with the elemental analysis, requiring a total of 3 equiv of non-coordinating water molecules.

Results and Discussion

Preparation and Characterization of Solid Materials. Solid materials of the taci complexes, having the composition M₃(H₋₃taci)₂X₃·*p*H₂O·*q*EtOH (M = Y, La, Eu, Gd, Dy; X = Cl, NO₃; 2.5 ≤ *p* ≤ 9; *q* = 0, 0.33) were prepared by a direct reaction in MeOH, using stoichiometric amounts of the metal salts and the ligand. In addition, three equiv of triethylamine were added for the deprotonation of the ligand. The tdc complexes M₃(H₋₃tdci)₂(NO₃)₃·*z*H₂O (M = Y, Eu; *z* = 7, 7.5) were prepared accordingly in water. Although the trinuclear complexes are formed exclusively in solution (see below), the yields of this procedure were moderate or even low (14–55%). The poor yields are not indicative of poor complex formation, but they must rather be attributed to the considerable difficulties encountered in obtaining pure, crystalline solids of a well-defined composition. The solid compounds were characterized by elemental analyses and FAB⁺ mass spectrometric measurements. A variety of pseudomolecular ions of the composition [M₃L₂X_{*p*} – *z*H]⁺ (L = taci, tdc; X = Cl, NO₃, H₂O, NBA) could be assigned in the mass spectrum, confirming the formation of the trinuclear M₃(H₋₃L)₂ unit (see Table S13, Supporting Information). For the Y, La, and the Eu complexes, a series of ¹H and ¹³C NMR spectroscopic measurements was performed. The spectra of the taci complexes in D₂O at pD 8 exhibited a total of two signals, which originate from the two types of protons –H(–C_O) and H(–C_N)– of the two cyclohexane rings. The signals could be assigned unambiguously by ¹H–¹³C HMQC and by saturation experiments assuming slow ligand exchange.²⁰ The stability of the La complex in D₂O (pD 7.6) appears to be comparably low, and partial decomposition of the complex was indicated by the emergence of the signals of free taci. This was, however, not the case for Y and Eu. Due to the paramagnetism of Eu^{III}, the signals of [Eu₃(H₋₃taci)₂]³⁺

were considerably shifted to lower frequency. For the tdc complexes, one singlet was observed for the twelve methyl groups. These characteristics are clearly indicative of the presence of one single complex in neutral or slightly alkaline aqueous solution, having full *D*_{3h} point symmetry.

Crystal Structures. Single-crystal X-ray diffraction experiments have been performed to elucidate the molecular structure of the La and the Gd complexes in the solid state.^{21,22} The crystal structure analyses confirmed the formation of the trinuclear [M₃(H₋₃taci)₂]³⁺ unit (Figure 1), where the three metal centers form an approximately equilateral triangle, which is encapsulated by the two triply deprotonated taci ligands. The same sandwich type structure has been observed for [Bi₃(H₋₃taci)₂]Cl₃·6H₂O.²⁴ In all these complexes, the taci ligands bind each metal center to an equatorial (eq) nitrogen and two axial (ax) oxygen atoms. The deprotonated oxygen atoms act as μ₂-alkoxo bridges while a terminal binding mode is found for the amino groups. Coordination of the metal center to the O_{ax}–N_{eq}–O_{ax} site results in the formation of one six-membered and two five-membered chelate rings. Each of the two taci ligands has a total of three such O_{ax}–N_{eq}–O_{ax} sites and all are occupied by the three metal centers. In contrast to the previously described Bi complex, where significantly different Bi–N bond lengths were observed for the two ligands, the La–N and Gd–N bonds are all of comparable length and the [M₃(H₋₃taci)₂]³⁺ fragment approaches *D*_{3h} point symmetry quite closely (Table 2).

Although the La and Gd complexes were both isolated as trichloride salts, they are not isostructural, and they differ in the amount of the incorporated water of crystallization. The Gd complex consists of discrete, trinuclear [Gd₃(H₋₃taci)₂(H₂O)₆]³⁺ cations (Figure 1) where six water molecules complete the coordination sphere of the three Gd atoms. The coordination sphere of each Gd atom thus consists of the four oxygen atoms of the bridging alkoxo groups, two primary amino groups and two peripheral water molecules giving a coordination number of 8. The coordination polyhedron can be described as a bicapped trigonal prism based on isosceles triangles. The two nitrogen atoms cap the two rectangular faces formed each by two alkoxo groups and the two water molecules. The [La₃–

(24) Hegetschweiler, K.; Ghisletta, M.; Gramlich, V. *Inorg. Chem.* **1993**, *32*, 2699.

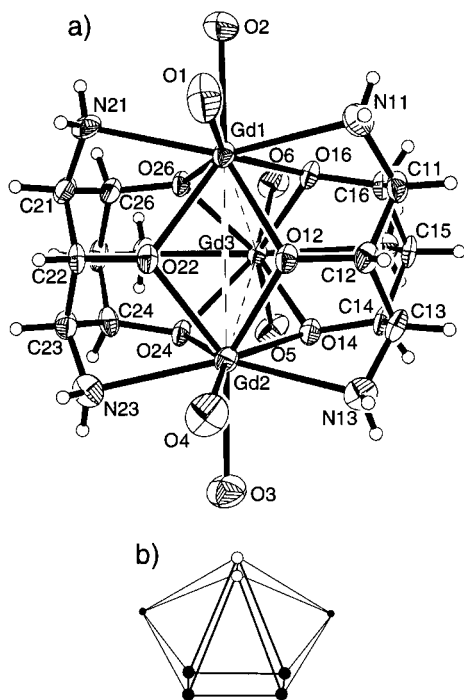


Figure 1. Structure of the trinuclear $[\text{Gd}_3(\text{H}_{-3}\text{taci})_2(\text{H}_2\text{O})_6]^{3+}$. (a) ORTEP representation with numbering scheme and vibrational ellipsoids at the 50% probability level. Hydrogen atoms are shown as spheres of arbitrary size. (b) Coordination polyhedron for Gd (large spheres, oxygen atoms, small spheres, nitrogen atoms). Closed spheres refer to the donor atoms of the taci-ligand, open spheres to peripheral water molecules. The La complex adopts a closely related structure, however, for two of the three La atoms, one of the peripheral water ligand is replaced by Cl^- .

$(\text{H}_{-3}\text{taci})_2]^{3+}$ cage adopts virtually the same structure, although the larger ionic radius of La^{3+} results in an elongation of the M–O, M–N, and $\text{M}\cdots\text{M}$ distances (Table 2). Moreover, a different arrangement of the peripheral ligands is observed. Only four water molecules are bound to the three metal centers. The remaining two positions are occupied by Cl^- anions, which in turn bridge two La atoms of two different complex molecules. This interconnecting structural motif results in the formation of indefinite chains which are oriented along axis *a*. The coordination polyhedra of the La centers are essentially the same as that observed for Gd; however, due to the different steric demands of Cl^- , the bicapped trigonal prism of the $\text{LaO}_5\text{N}_2\text{Cl}$ moiety is considerably distorted.

In classical coordination compounds of the lanthanoid cations, coordination numbers of 6 to 12 are known,²⁵ and the observed coordination number of 8 is not unusual, although the most frequently observed coordination number for La^{III} and Gd^{III} , is 9.^{26,27} For the lanthanoid(III) aqua ions, the coordination number changes along the series from 9 at the beginning to 8 at the end, with an equilibrium for Sm^{3+} .²⁸

The M–N and M–O bond distances of the two $[\text{M}_3(\text{H}_{-3}\text{taci})_2]^{3+}$ complexes lie all within the ranges expected for a coordination number of eight.^{29,30} It is, however, noteworthy that different M–O bond distances are observed for the alkoxo groups of the taci ligand and for H_2O (Table 2), with the M–OH₂ distances considerably longer.

It has been shown previously that taci can bind a metal center either in a symmetric manner with three axial substituents, or asymmetrically, with three substituents having a consecutive axial–equatorial–axial (ax–eq–ax) arrangement.⁷ According to molecular mechanics calculations, the steric demands of the two binding modes are distinctly different.³¹ The syn-triaxial binding mode results in an adamantane like structure which is favorable for small metal cations. For larger cations, however, the asymmetric binding mode is energetically more favored. Comparing the strain energy of the two binding modes ($N_{\text{ax}}-N_{\text{ax}}-N_{\text{ax}}$ versus $O_{\text{ax}}-N_{\text{eq}}-O_{\text{ax}}$) as a function of metal ion size, an intersection at about 0.8 Å is found. With regard to the steric properties, large cations should thus bind preferentially to the asymmetric $O_{\text{ax}}-N_{\text{eq}}-O_{\text{ax}}$ site. The observed structures of the La and Gd complex agree well with this prediction.

Magnetism of the Gd Complex. Magnetic coupling interactions between the three Gd centers of $[\text{Gd}_3(\text{H}_{-3}\text{taci})_2(\text{H}_2\text{O})_6]^{3+}$ were investigated by magnetic measurements in the temperature range of 2.3–60 K using a SQUID magnetometer. The magnetic susceptibility and the effective magnetic moment per Gd atom as a function of temperature are depicted in Figure S2 (Supporting Information). At 60 K, a magnetic moment of $7.8 \mu_{\text{B}}$ is observed, a value which corresponds closely to the spin-only value of the uncoupled $4f^7$ center ($7.94 \mu_{\text{B}}$). On lowering the temperature to 2.3 K this value decreased to $5.98 \mu_{\text{B}}$, indicating that weak antiferromagnetic interactions are active. The magnetic susceptibility was reproduced using the standard formulas for a trinuclear complex.³² Due to the approximate D_{3h} point symmetry, equal exchange pathways between the metal centers were assumed and one single value was used for the coupling constants within the Gd_3 triangle. Using least-squares calculations, the experimental data could be fitted with $J = -0.092 \text{ cm}^{-1}$ and $g = 1.98$. The coupling constant evaluated from the fitting procedure is very small. The low-energy of the coupling interactions must be attributed to the small overlap between the $4f$ orbitals of Gd and the μ -alkoxo bridges. However, the coupling is still significantly larger than the evaluated dipole contribution $J_{\text{dip}} = g^2\mu_{\text{B}}^2r^{-3} = -0.033 \text{ cm}^{-1}$.

Our findings differ from those reported by Aspinall et al. where a considerable lowering of the magnetic moment was observed for a trinuclear alkoxo bridged Gd^{III} complex even at room temperature.²⁷ They are, however, in excellent agreement with the observation of Benelli et al.³³ and Orvig and co-workers,³⁰ who observed very weak antiferromagnetic coupling interactions for dinuclear μ -alkoxo- or μ -phenoxo-bridged Gd^{III} complexes.

- (25) (a) For Gd^{III} with coordination number of 6, see: Liu, S.; Yang, L.-W.; Rettig, S. J.; Orvig, C. *Inorg. Chem.* **1993**, *32*, 2773. (b) For La^{III} with coordination number of 12, see: Arif, A. M.; Gray, C. J.; Hart, F. A.; Hursthouse, M. B. *Inorg. Chim. Acta* **1985**, *109*, 179.
- (26) (a) Kumar, K.; Chang, C. A.; Francesconi, L. C.; Dischino, D. D.; Malley, M. F.; Gougoutas, J. Z.; Tweedle, M. F. *Inorg. Chem.* **1994**, *33*, 3567. (b) Casellato, U.; Tamburini, S.; Tomasin, P.; Vigato, P. A.; Botta, M. *Inorg. Chim. Acta* **1996**, *247*, 143. (c) Kang, S. I.; Ranganathan, R. S.; Emswiler, J. E.; Kumar, K.; Gougoutas, J. Z.; Malley, M. F.; Tweedle, M. F. *Inorg. Chem.* **1993**, *32*, 2912. (d) Chang, C. A.; Francesconi, L. C.; Malley, M. F.; Kumar, K.; Gougoutas, J. Z.; Tweedle, M. F.; Lee, D. W.; Wilson, L. J. *Inorg. Chem.* **1993**, *32*, 3501. (e) Konings, M. S.; Dow, W. C.; Love, D. B.; Raymond, K. N.; Quay, S. C.; Rocklage, S. M. *Inorg. Chem.* **1990**, *29*, 1488.

- (27) Aspinall, H. C.; Black, J.; Dodd, I.; Harding, M. M.; Winkley, S. J. *J. Chem. Soc., Dalton Trans.* **1993**, 709.
- (28) (a) Cossy, C.; Helm, L.; Powell, D. H.; Merbach, A. E. *New J. Chem.* **1995**, *19*, 27. (b) Kowall, T.; Foglia, F.; Helm, L.; Merbach, A. E. *Chem. Eur. J.* **1996**, *2*, 285.
- (29) Andruh, M.; Bakalbassis, E.; Kahn, O.; Trombe, J. C.; Porcher, P. *Inorg. Chem.* **1993**, *32*, 1616.
- (30) Liu, S.; Gelmini, L.; Rettig, S. J.; Thompson, R. C.; Orvig, C. *J. Am. Chem. Soc.* **1992**, *114*, 6081.
- (31) Hegetschweiler, K.; Wörle, M.; Meienberger, M. D.; Nesper, R.; Schmalte, H. W.; Hancock, R. D. *Inorg. Chim. Acta* **1996**, *250*, 35.
- (32) (a) Kambe, K. *J. Phys. Soc. Jpn.* **1950**, *5*, 48. (b) Cannon, R. D.; White, R. P. *Prog. Inorg. Chem.* **1988**, *36*, 195.
- (33) Benelli, C.; Guerriero P.; Tamburini, S.; Vigato, P. A. *Mater. Chem. Phys.* **1992**, *31*, 137.

Table 3. Evaluated Formation Constants^a for [M₃(H₋₃taci)₂]³⁺, [M₃(H₋₃taci)(OH)]⁵⁺, and [Eu₃(H₋₃taci)₂(OH)]²⁺ (M = Y, Eu, Gd, Dy, Lu)

	Y ^{III}	Eu ^{III}	Gd ^{III}	Dy ^{III}	Lu ^{III}
method ^b	batch	cont	cont	batch	batch
log β _{xyz} ^c					
x y z					
3 2 -6	-16.4 ± 0.1	-18.5 ± 0.1	-18.2 ± 0.1	-14.6 ± 0.1	-11.3 ± 0.1
3 2 -7		-29.5 ± 0.2			
3 1 -4 ^d	-12.0 ± 0.3				-8.7 ± 0.2
σ _{pH} ^d	0.0106	0.0036	0.0087	0.0082	0.0108

^a 0.1 M KCl, 25 °C. ^b Type of titration (continuous or batchwise, see Experimental section). ^c β_{xyz} = [H_zM_x(taci)_y][H]^{-z}[taci]^{-y}[M]^{-x}. ^d See ref 37.

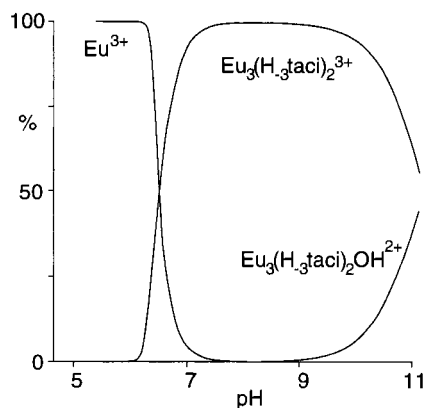
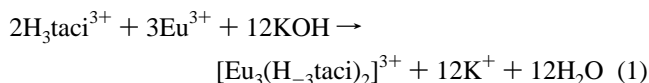


Figure 2. Species distribution in an equilibrated solution of [Eu₃(H₋₃taci)₂]Cl₃. The distribution is calculated for a total Eu concentration of 1.5 mM and a total taci concentration of 1.0 mM. The formation constants listed in Table 3 were used for the calculations. Only metal-containing species are shown.

Equilibria and Species Distribution in Aqueous Solution.

The stoichiometry of the species formed in aqueous media and the corresponding formation constants were investigated by pH-metric titrations (Table 3). The Eu–taci system was chosen for a comprehensive study, as the favorable properties of Eu^{III} afford for a parallel NMR investigation. On the other hand, Eu and Gd are neighbors in the lanthanoid series, and the stability constants obtained for Eu will be applicable for Gd as well. The Eu-to-ligand ratio was varied systematically from 1:2 to 3:2 to ensure that all possible species were considered. A survey of the titration curves is shown in Figure S3 (Supporting Information). These experiments established unambiguously that the trinuclear [M₃(H₋₃taci)₂]³⁺ which formed according to the eq 1



is the only metal containing species in the range of 7 ≤ pH ≤ 9 (Figure 2). The titration curves can be divided into four distinct regions. In a first step (pH < 6.2) addition of base removed one proton from H₃taci³⁺. Further addition of base resulted in the formation of the complex. The formation of a polynuclear species is clearly indicated by the very low slope of the pH curve in this range. In a third part, excess H₂taci²⁺ is deprotonated and this region of the curve simply corresponds to the neutralization of the ligand. Finally, at high pH, further deprotonation of the complex must be considered to fit the experimental data. The species formed was tentatively formulated as a hydroxo complex [Eu₃(H₋₃taci)₂(OH)]²⁺ (deprotonation of one of the peripheral water ligands). There is, however, some evidence that at the end of the titration, a subsequent hydrolytic polymerization reaction occurs, resulting in the

formation of species of higher degree of deprotonation and also of higher nuclearity.

A corresponding ¹H NMR study in D₂O confirmed the results obtained by the pH-metric measurements. A Eu³⁺:taci ratio of 1:3 up to 1:25 was used. The ligand was added in its triply protonated form as [H₃taci]Cl₃ and the pD of the samples were varied systematically by adding NaOD to the sample solution. During data acquisition, the relaxation delay was increased to about 10 s, to allow a quantitative evaluation of the integrated spectra.³⁴

The results of this NMR study for the Eu-taci system are as follows:

(i) A maximum of four signals could be observed for all samples. They could be assigned to the excess of the free taci ligand and to the same Eu complex as already obtained by simple dissolution of solid [Eu₃(H₋₃taci)₂]Cl₃ in D₂O.²⁰

(ii) Both the free ligand and the complex always exhibited separate signals. Complex formation is thus sufficiently slow to allow the observance of individual species by the NMR experiments at room temperature.

(iii) Because of the excess of taci, signals corresponding to the free ligand were always present in the spectrum. However, signals of the complex were only observed above pD 5.5. This pD dependence of the degree of complex formation is in excellent agreement with the species distribution calculated from the potentiometric data (Figure 2). The corresponding comparison of the amount of metal bonded taci observed in the ¹H NMR spectra³⁴ at different pD with the expected formation of [Eu₃(H₋₃taci)₂]³⁺ in D₂O is shown in Figure S4 (Supporting Information).

(iv) The signals of the free taci showed the pD dependence as expected for a tribasic amine with pK_a values of 5.95, 7.40, and 8.90.^{17,35} However, the signals of the complex exhibited no change of the chemical shift in the range 6 ≤ pD ≤ 10.

(v) Above pD 11, a linear increase was observed in the chemical shifts of the complex signals with increasing pD. Additional signals could, however, not be detected. These characteristics are indicative of equilibration that is fast with respect to the NMR time scale with averaged signals being observed for the different species. Such a fast reaction is again in good agreement with the results of the potentiometric study, where a deprotonation of a coordinated water molecule was postulated to occur at high pH.

(vi) Even at very high taci concentration (25-fold excess) there was no indication of the formation of complexes with a higher

(34) The T₁ relaxation times of the two ring protons of taci were determined by an inversion recovery experiment. Values of 2.06 s for H(–C_O) and 1.10 s for H(–C_N) were found. A pulse delay of 10 s thus ensured complete relaxation and allowed a quantitative evaluation of the integrated spectrum.

(35) It should be noted that slightly different pK_a values are expected for D₂O. Using the pD dependence of the chemical shifts of taci, corresponding values of 6.07, 7.32, and 8.84 were calculated by a least-squares refinement (32 data points) as described in ref 7.

taci:Eu ratio than 2:3. Thus, the simple mononuclear complexes such as $[M(\text{taci})]^{2+}$ and $[M(\text{taci})_2]^{2+}$ which are well established for many 3d transition-metal and group 12 cations^{7,17,36} do not form with Eu^{3+} . The sandwich-type $\text{M}_3(\text{H}_{-3}\text{taci})_2$ cage seems thus to represent a particularly favorable structure for this cation.

For comparison, the Eu–tdci system (tdci = 1,3,5-trideoxy-1,3,5-tris(dimethylamino)-*cis*-inositol, Chart 1) has also been studied. Complex formation was too slow to be investigated by continuous titration. Consequently, a batch experiment was performed to determine the formation constant. A value of -16.8 ± 0.3 was evaluated for $\log \beta_{32-6}$ ($\beta_{32-6} = [\text{M}_3(\text{H}_{-3}\text{L})_2] \cdot [\text{M}]^{-3} \cdot [\text{L}]^{-2} \cdot [\text{H}]^6$). This value is somewhat less negative than the corresponding value for taci ($\log \beta_{32-6} = -18.5 \pm 0.1$) and indicates that the stability of the tdci complex is increased by about 2 orders of magnitudes.

Additional potentiometric titration experiments were performed to investigate complex formation of taci with Y^{3+} , Gd^{3+} , Dy^{3+} , and Lu^{3+} (Table 3). An M:taci ratio of 3:2 was used in all experiments. The measurements with Gd^{3+} could be performed by a continuous titration experiment. However, the kinetics of complex formation with Y^{3+} , Dy^{3+} , and Lu^{3+} proved to be too slow for this method and the batch procedure was applied. The potentiometric data could all be evaluated assuming the formation of the trinuclear $[\text{M}_3(\text{H}_{-3}\text{taci})_2]^{3+}$ as the main component. For Gd^{3+} and Dy^{3+} there was no indication of any other metal complexes. However, for Y^{3+} and Lu^{3+} some evidence was found that $[\text{M}_3(\text{H}_{-3}\text{taci})(\text{OH})]^{5+}$ was formed as an additional minor species.³⁷

The stability of the $[\text{M}_3(\text{H}_{-3}\text{taci})_2]^{3+}$ complexes increases monotonically within the lanthanoids and the log of the formation constant can approximately be expressed as a simple linear function of the ionic radius (Figure 3). This is not valid for the Y^{3+} complex, where considerable deviation is observed from this correlation. In agreement with this increase of stability with increasing atomic number of the lanthanoids, the La complex itself proved to be of rather low stability. This is indicated by a partial dissociation after dissolution of the solid complex in D_2O . In contrast, no significant liberation ($\leq 1\%$) of free taci has been observed in the NMR spectra of the Y and Eu complexes in the range $7 \leq \text{pD} \leq 8$. Due to the low stability of the La complex, and the consequent precipitation of $\text{La}(\text{OH})_3$ at increasing pH, it was not possible to obtain a quantitative determination of the formation constant by potentiometric titration.

A similar monotonical increase of stability with increasing atomic number as reported here for the trinuclear taci complexes

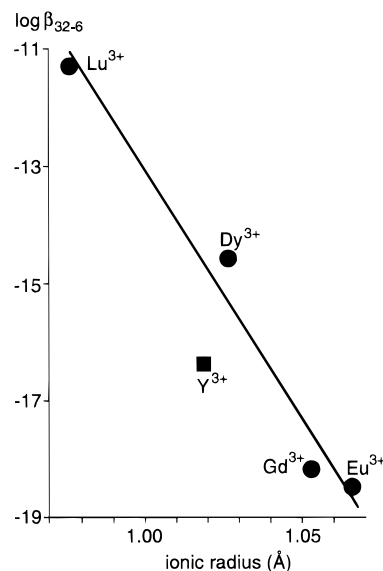


Figure 3. The $\log \beta_{32-6}$ values ($\beta_{32-6} = [\text{M}_3(\text{H}_{-3}\text{L})_2] \cdot [\text{M}]^{-3} \cdot [\text{L}]^{-2} \cdot [\text{H}]^6$) for various metal cations as a function of metal ion radius. The ionic radii were taken from ref 38.

Table 4. pM (= $-\log [\text{M}^{3+}]$) Values for a Variety of Lanthanoid Complexes for Conditions as Indicated^a

complex	M_T, L_T^b	pM: pH 7.4, pH 8.0	reference ^c
$[\text{Eu}_3(\text{H}_{-3}\text{taci})_2]^{3+}$	10, 6.667	4.90, 6.30	this work
$[\text{Eu}_3(\text{H}_{-3}\text{tdci})_2]^{3+}$	10, 6.667	4.92, 6.41	this work
$[\text{Gd}_3(\text{H}_{-3}\text{taci})_2]^{3+}$	10, 6.667	5.01, 6.43	this work
$[\text{Gd}(\text{dtpa})]^{2-}$	10, 10	10.01, 10.64	39
$[\text{Gd}(\text{dtpa-bma})]$	10, 10	8.44, 8.73	39
$[\text{Gd}(\text{dota})]^-$	10, 10	10.41, 12.58	40, 26a

^a dtpa, diethylenetrinitriolpentaacetate; dtpa-bma, diethylenetrinitriolpentaacetate-bis(methyl)amide; dota, 1,4,7,10-tetraazacyclododecane-*N,N',N'',N'''*-tetraacetate. ^b Total metal and total ligand concentration ($10^{-3} \text{ mol dm}^{-3}$). ^c For the formation constants used.

of the lanthanoids is also observed for the Ln–edta complexes. However, for other polyamino-polycarboxylates such as dota and dtpa, different behavior has been reported. The stability of these complexes increases only monotonically until Gd and then remains largely constant for the later cations of this series.¹⁶

Conclusions

The taci complexes with trivalent lanthanoid ions exhibit a compact, sandwich-type cage structure of the composition $[\text{M}_3(\text{H}_{-3}\text{taci})_2]^{3+}$. In the solid state, each of the metal centers is coordinated to two additional peripheral ligands such as H_2O or a counterion. The presence of the $[\text{M}_3(\text{H}_{-3}\text{taci})_2]^{3+}$ unit in aqueous solution has been demonstrated by NMR spectroscopic and potentiometric measurements.

In the context of MRI, the potential of $[\text{Gd}_3(\text{H}_{-3}\text{taci})_2(\text{H}_2\text{O})_6]^{3+}$ as a contrast agent is clearly limited by its low stability (Table 4). However, it is an interesting model molecule which allows to study the effects of intramolecular Gd–Gd interaction on electronic relaxation, and consequently on proton relaxivity.⁸ According to the evaluated species distribution shown in Figure 2 the trinuclear complex decomposes immediately if the pH falls below 6. This inability of taci to bind lanthanoid cations in acidic aqueous media is based on the very unfavorable proton balance of the formation reaction as expressed in eq 1. In alkaline media, the trinuclear complexes of Y^{3+} , Eu^{3+} , Gd^{3+} , Dy^{3+} , and Lu^{3+} proved to be stable (Figure 2 and Table 4).

An increase in complex stability can be achieved by synthetic modification of the taci ligand. As an example, we have

(36) Hegetschweiler, K.; Hancock, R. D.; Ghisletta, M.; Kradolfer, T.; Gramlich, V.; Schmalte, H. W. *Inorg. Chem.* **1993**, *32*, 5273.

(37) Inspection of the calculated and measured pH values in the alkalimetric titration showed some systematic deviation in the early range of metal complex formation. A variety of different models with additional species were tested to account for this phenomenon. Most satisfying results were obtained by the consideration of a complex, having the composition $[\text{H}_{-4}\text{M}_3(\text{taci})]^{5+}$. For Y^{III} , $\sigma_{\text{pH}} = (\sum w(\text{pH}_{\text{obs}} - \text{pH}_{\text{calc}})^2 / \sum w)^{1/2}$; $w = (\text{pH}_{i+1} - \text{pH}_{i-1})^{-2}$ decreased from 0.0134 to 0.0106 and for Lu^{III} from 0.0178 to 0.0108. In accordance with the observations, found previously for the trinuclear Pb^{II} taci complex (ref 24), we tentatively assign a corresponding half sandwich structure $[\text{M}_3(\text{H}_{-3}\text{taci})(\text{OH})]^{5+}$ with a μ_3 -hydroxo ligand to this complex. The evaluation showed, however, that it appeared only as minor species ($< 20\%$) and its composition and stability could therefore not be established with the same unambiguousness as for the main component. Moreover, the presence or absence of the minor species did not change the evaluated formation constants of the main $[\text{M}_3(\text{H}_{-3}\text{taci})_2]^{3+}$ within the experimental error.

(38) Shannon, R. D. *Acta Crystallogr.* **1976**, *A32*, 751.

(39) Cacheris, W. P.; Quay, S. C.; Rocklage, S. *Magn. Reson. Imaging* **1990**, *8*, 467.

(40) Kumar, K.; Tweedle, M. F. *Inorg. Chem.* **1993**, *32*, 4193.

demonstrated in this study, that the corresponding Eu–tdci complex is almost 2 orders of magnitude more stable. It is well-known that tdc complexes with an analogous structure are generally of higher stability than the corresponding taci complexes.¹³ A further stability enhancement could be achieved by connecting the two taci frameworks by an N–(CH₂)₂–NH–(CH₂)₂–N or N–(CH₂)₂–O–(CH₂)₂–N bridge or by introducing substituents onto the nitrogen atoms which carry additional donor groups. We are currently investigating such modifications in our laboratory.

Acknowledgment. We thank Dr. Peter Osvath (CSIRO, Clayton, VIC, Australia) for his careful reading of the manuscript. Financial support from the Swiss National Science Foundation to R.H., from the Kredite für Unterricht und

Forschung der ETH Zürich to M.G. and from Nycomed Inc. to E.T. and A.E.M. is gratefully acknowledged. This research was carried out in the frame of the EC COST D8 Action and the EU-BIOMED Program (MACE project).

Supporting Information Available: Listings of crystallographic data, anisotropic displacement parameters, positional parameters of hydrogen atoms, bond distances and bond lengths, FAB⁺ MS data, and potentiometric data and figures showing an ORTEP representation of the La complex, magnetic properties of the Gd complex as a function of T, calculated and observed titration curves and the pD-dependent formation of [Eu₃(H–₃taci)₂]³⁺ in D₂O (¹H NMR) (12 pages). Ordering information is given on any current masthead page.

IC980685S